



Low-Backscatter Ocean Features in Synthetic Aperture Radar Imagery

Pablo Clemente-Colón and Xiao-Hai Yan

Many ocean surface signatures in synthetic aperture radar (SAR) imagery are characterized by relatively low normalized radar cross section values. Distinguishing among these signatures objectively can be very difficult, especially with only the single-band and single-polarization SAR imagery available from the European Remote Sensing satellites and the Canadian Radarsat-1. Nevertheless, distinctive patterns, when interpreted in the context of the geographic region, season, and local weather conditions, can be extremely useful in properly identifying many of the observed low-backscatter features. Examples of such features presented here are interpreted based on the regional and temporal context of the SAR imagery as well as the morphology and temporal persistence of the features. (Keywords: Low backscatter, Low wind, Oil slicks, Surfactant, Upwelling.)

BACKGROUND

For this review, we define low-backscatter ocean features simply as those features imaged by synthetic aperture radar (SAR) over the ocean that are characterized by relatively low normalized radar cross section (NRCS) values within a scene. NRCS is a measure of the radar energy scattered back toward the radar (in decibels) and is independent of the image resolution or pixel size. In contrast to most SAR imaging of land or sea ice surfaces, where a predetermined surface roughness is present, wind is essential in establishing the surface roughness (wind waves) necessary for most SAR imaging of ocean features. The viewing geometry along with the radar wavelength and polarization used are also fundamental factors in determining the observed ocean NRCS.

Bragg Wave Modulation

The ocean surface roughness responsible for the backscatter energy detected by radar is produced primarily by the capillary and small gravity waves generated by the local wind. According to the Bragg model, the radar microwaves are in resonance with ocean waves of similar scale.¹ These so-called Bragg waves are related to the radar wavelength by

$$\lambda_o = \lambda_r / 2 \sin \theta ,$$

where λ_o is the ocean waves wavelength, λ_r is the radar wavelength, and θ is the angle of the radar wave at the ocean surface or incidence angle. Bragg waves can be further modulated by the longer waves on which they ride through tilt and hydrodynamic effects.² The long

wave spectrum itself usually responds to the wind conditions as well.

Atmospheric processes that affect surface wind conditions, and thus the generation and modulation of Bragg waves, as well as oceanic processes that directly modulate the Bragg wave spectrum produce signatures readily imaged by SAR. In general, lower wind speeds generate fewer Bragg waves. This produces a smoother ocean surface that appears in the SAR imagery as areas of relatively low NRCS. Below a low wind speed threshold, SAR scenes will have such low NRCS values that features dependent on the modulation of Bragg waves to be imaged will not be visible.

Viewing Geometry

SAR incidence angle and look direction with respect to the wind are crucial factors in determining the NRCS. Sea surface backscatter decreases rapidly with increasing radar incidence angle. As a consequence, SAR is generally brighter in the near range and darker in the far range. Success in detecting low-backscatter ocean features may well depend on where the features lie within a scene swath. Location is of special significance for Radarsat wide swath SAR imagery, which can have a range width of up to 500 km and incidence angles varying from 20 to 50°. The wider the swath, the greater the contrast between the near-range and far-range NRCS. Lower NRCS in the far range makes the detection and identification of low-backscatter features difficult at that range. The wind direction relative to the satellite view also affects the observed NRCS in a scene. A crosswind (wind blowing perpendicular to the range direction) produces lower NRCS values than an upwind or downwind (wind blowing along the range direction) owing to the different orientation of the wind wave facets in each case.

Wavelength and Polarization

The wavelength of the Bragg waves and the observed NRCS are a function of the radar wavelength. Depending on the scale of the process and the wind conditions, imagery obtained at one radar wavelength may strongly detect a low-backscatter feature in a scene while imagery obtained at another wavelength may not. For example, SAR L-band sensors are sensitive to processes that modulate surface waves at the decimeter scale while C-band SAR sensors are sensitive to centimeter-scale Bragg waves. The observed NRCS is also a function of the send-and-receive polarization used by the radar system. The Shuttle Imaging Radar (SIR) missions have shown the potential of combining multi-band and multipolarization spaceborne observations in improving low-backscatter feature identification. Unfortunately, today's satellite SAR systems are limited to a single band and a single polarization.

A characterization of the feature morphology, geographic and temporal context, and local ocean and atmospheric weather conditions is critical to properly identify many of the observed features. Atmospheric and ocean processes are both involved in the imaging of the low-backscatter features discussed in the next section. In general, these features reflect either meteorological or oceanographic conditions.

METEOROLOGICAL FEATURES

Low Surface Winds

Given the dependence of sea surface roughness on the wind, the most conspicuous feature imaged by SAR over the ocean is the wind speed variability itself. Atmospheric circulation produces and also can further modulate the Bragg waves. SAR images provide a view of the high variability of atmospheric mesoscale and submesoscale circulation processes at the marine boundary-layer level.

One interesting example of this phenomenon is the signature of a tropical convective system imaged using Radarsat ScanSAR wide mode observed south of Saint Croix Island (Fig. 1a). Atmospheric circulation variability produces the most common low-backscatter ocean features imaged by SAR, i.e., areas of relatively low wind speed. Atmospheric gravity waves and boundary-layer rolls affect the local wind conditions, producing distinctive quasi-periodic dark (low wind speed) and bright (high wind speed) patterns in SAR images. Figure 1b shows the signature of atmospheric internal gravity waves generated off the East Coast of the United States. The spatial scale of these waves (about 500 m in this case) separates them from other atmospheric or oceanic phenomena. Areas of wind shadowing by coastal topography or man-made obstacles are also commonly imaged by SAR. Good examples of wind shadowing are produced when wind blowing from the Bering Sea is blocked by the high topographic relief of the Aleutian Islands, as seen in Fig. 1c.

Rain Effects

Rain may produce low-backscatter signatures in SAR imagery through two distinct processes. First, atmospheric attenuation due to volume scattering will tend to decrease the total NRCS observed over an area under a rain system. Second, depending on the wind speed and Bragg wave scale, raindrop impact on the sea surface may tend to dampen the Bragg waves and thus reduce the NRCS of the impacted region. The relative importance of each of these processes in lowering backscatter is a function of the radar wavelength, rain rate, and wind speed.³ Whereas a C-band sensor is affected more by rain volume scattering, an L-band sensor is more sensitive to a decrease in backscatter due to Bragg

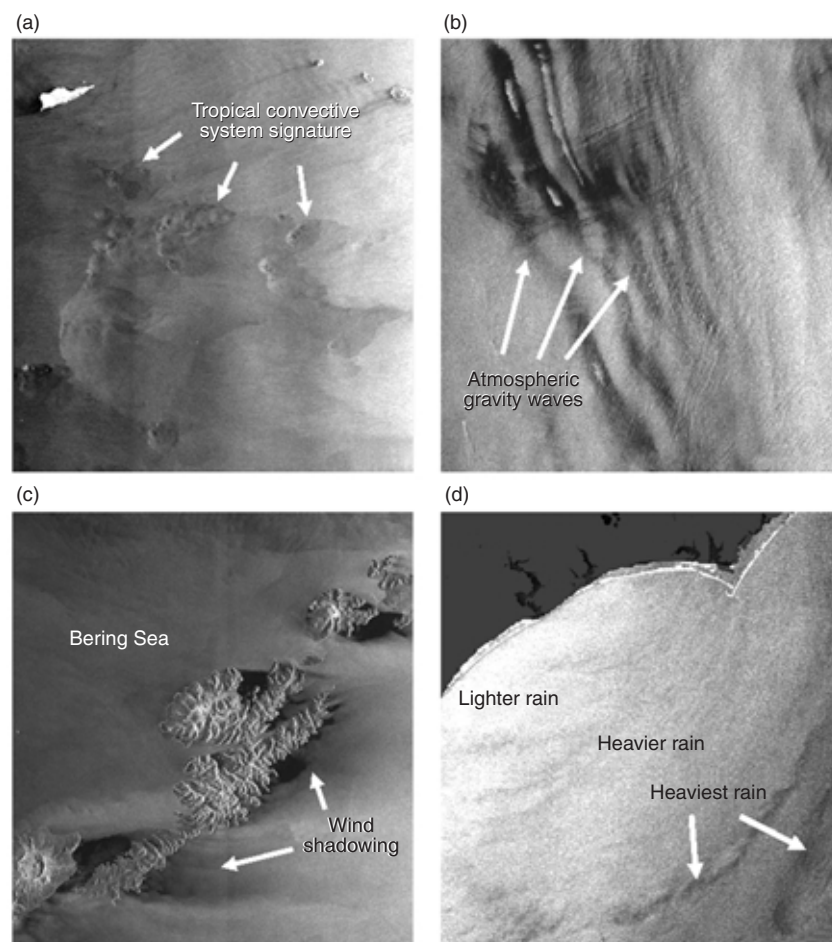


Figure 1. Radarsat images illustrating various meteorological features. (a) ScanSAR wide subimage of the Eastern Caribbean Sea south of Saint Croix, U.S. Virgin Islands, showing the signature of a tropical convective system on 24 July 1997 at 1009 UT; (b) standard mode SAR subimage showing atmospheric internal gravity wave patterns off the U.S. East Coast on 3 July 1998 at 1111 UT; (c) ScanSAR wide subimage showing shadowing effects produced as wind blows over the Aleutian Islands from the Bering Sea into the Gulf of Alaska on 20 February 1998 at 1729 UT; and (d) ScanSAR wide subimage showing decreased backscatter under regions of increased rainfall as Hurricane Bonnie hits the coast of North Carolina on 27 August 1998 at 1108 UT. (© Canadian Space Agency, 1997, 1998.)

wave damping by the rain. The effect of rain attenuation in a hurricane is shown in Fig. 1d. Increased rain rates over regions of decreased backscatter were confirmed by regional NEXRAD observations at the time of the SAR image (see Friedman and Li, this issue; also Katsaros et al., this issue).

OCEANOGRAPHIC FEATURES

Surfactants

Surfactants as a whole are perhaps the most popularly recognized oceanographic low-backscatter features imaged by SAR. These substances can be divided into two major categories: natural and man-made. Each category can be further subdivided into those of biogenic and those of mineral origin. Natural biogenic slicks are produced by plankton and fish substances normally

released into the environment. Natural mineral slicks are the result of ocean-bottom oil seeps such as those found in the Gulf of Mexico or the Santa Barbara Channel off southern California. Man-made mineral slicks are typically caused by accidental spills or the illegal dumping of petroleum products; man-made biogenic slicks are produced by the discharge of organic matter resulting from human activities such as fish processing.

Surfactants are very effective at damping the wind generation of Bragg waves and can produce filaments or more extended regions of low NRCS in the SAR imagery.^{4,5} Under moderate wind conditions, these features can be detected by their contrast with the background NRCS. At higher wind speeds (over 5 to 6 m/s), surfactants at the surface layer will tend to mix down into the water column and become undetectable by SAR. At wind speeds below 2 m/s, the background NRCS becomes extremely low, the required contrast is effectively lost, and the slicks become essentially undetectable by SAR.

Figure 2a shows the effect of wind speed changes across an atmospheric front on the imaging of oil seep slicks in the Gulf of Mexico. High wind conditions decrease the detection of slicks above the front while lower wind conditions allow for the imaging of numerous

slick features below the front. An example of natural biogenic slicks resulting from enhanced biological activity during upwelling off the Delaware Bay is shown in Fig. 2b. Slicks associated with bilge pumping activities in the La Plata estuary off Uruguay are shown in Fig. 2c, and slick patterns produced by walleye pollack trawl fishing operations in the Bering Sea are seen in Fig. 2d.

Sea Ice

Sea ice impacts the NRCS mostly through non-Bragg effects. Specifically, SAR is sensitive to the surface roughness, internal structure, salinity content, and wetness of sea ice. First-year ice floes, for example, have a relatively smooth surface and a high salinity content. These factors cause radar energy to be reflected away

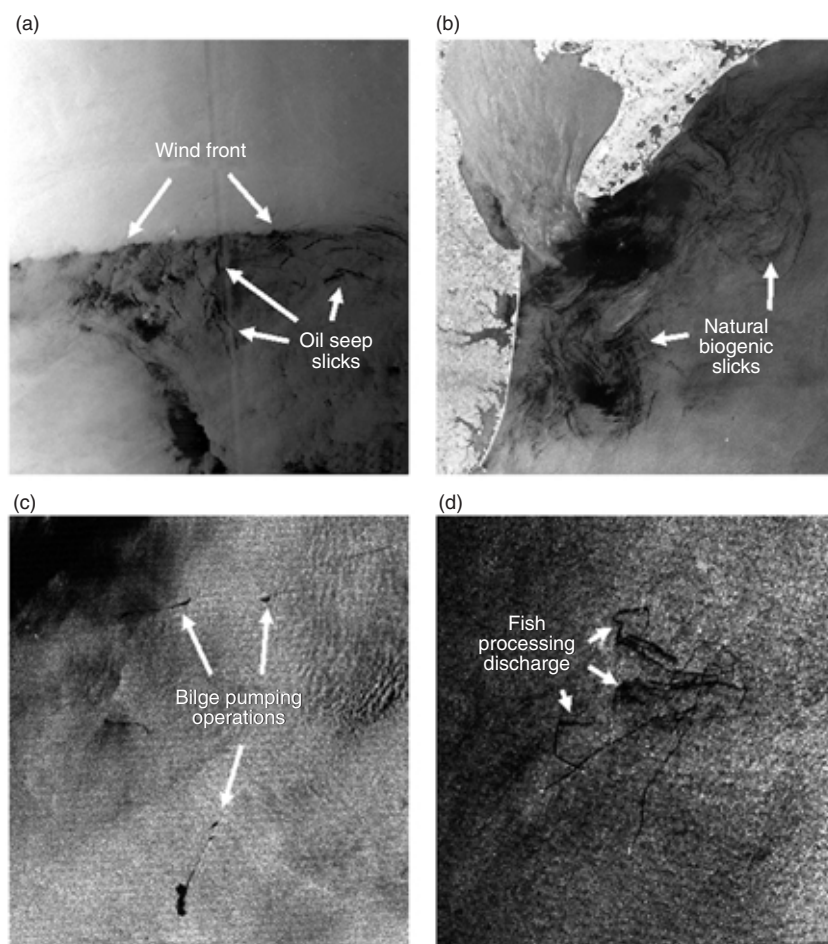


Figure 2. Radarsat images illustrating various oceanographic features. (a) ScanSAR wide image of a wind speed front and oil seep slicks in the Gulf of Mexico on 23 November 1997 at 0009 UT; (b) standard mode SAR image of the Delaware Bay region showing slicks associated with biological activity on 16 July 1998 at 2248 UT; (c) ScanSAR narrow subimage of the La Plata estuary off the coast of Uruguay showing slicks associated with suspected bilge pumping operations on 26 February 1997 at 0900 UT; and (d) ScanSAR wide subimage of the Bering Sea showing slick patterns produced by trawl fishing operations on 3 September 1997 at 1825 UT. (© Canadian Space Agency, 1997, 1998.)

from the sensor, thereby producing relatively low-backscatter signatures in SAR imagery when compared to surrounding brash or rougher multi-year ice.

Sea ice can also dampen ocean surface waves. In particular, grease ice (composed of small millimeter-sized crystals that form when seawater begins to freeze) dampens Bragg waves and produces areas of extremely low NRCS. As it accumulates on the sea surface, grease ice forms slick patterns similar to those produced by mineral or biogenic surfactants. An example of grease ice formed off the ice edge in the Bering Sea is shown in Fig. 3a. Proximity to the ice edge provides a good indication of the nature of these features.

Upwelling

Upwelling occurs when a divergent surface flow, commonly driven by the wind, is compensated by an

onshore deeper flow that brings colder and nutrient-rich water to the surface. Changes in the stability of the marine boundary layer due to changes in the air-sea temperature difference over the upwelling region, and hence in the efficiency of Bragg wave generation, have a direct effect on the observed backscatter.⁶ The increased stability produced by lower sea surface temperature results in lower wind stress and a decrease in available Bragg scattering waves, producing an overall decrease in NRCS over the region. The lower temperature of the upwelled waters is also responsible for an increase in the viscosity of the surface layer. This, in turn, affects the damping and initiation of Bragg waves and thus can also decrease NRCS.⁷ As mentioned earlier, enhanced biological activity, caused by high-nutrient waters, also produces an abundance of natural biogenic slicks that can be detected by SAR in an upwelling area. The combined effect of all of these processes produces a marked decrease in NRCS in an area dominated by upwelling, as seen in Fig. 2b.

Other Oceanographic Features

As in the case of the atmosphere, variations in the ocean surface circulation also modulate

the Bragg wave spectrum. Internal gravity waves in the ocean can affect the local sea surface velocities and thus the Bragg wave spectrum. This modulation allows for the internal waves to be imaged by SAR, as seen in Fig. 1d. Internal waves can also concentrate surfactants and may appear as distinctive periodic dark bands in SAR imagery. Surfactants can accumulate at convergence zones and along ocean current shear fronts, often delineating such circulation patterns.⁸ In addition, extremely shallow regions such as mudflats at low tide can produce very smooth surface conditions that appear as dark features in SAR imagery.

FEATURE CHARACTERIZATION

Several parameters can be used to characterize and distinguish low-backscatter ocean features, including the NRCS, morphology, geographical and temporal

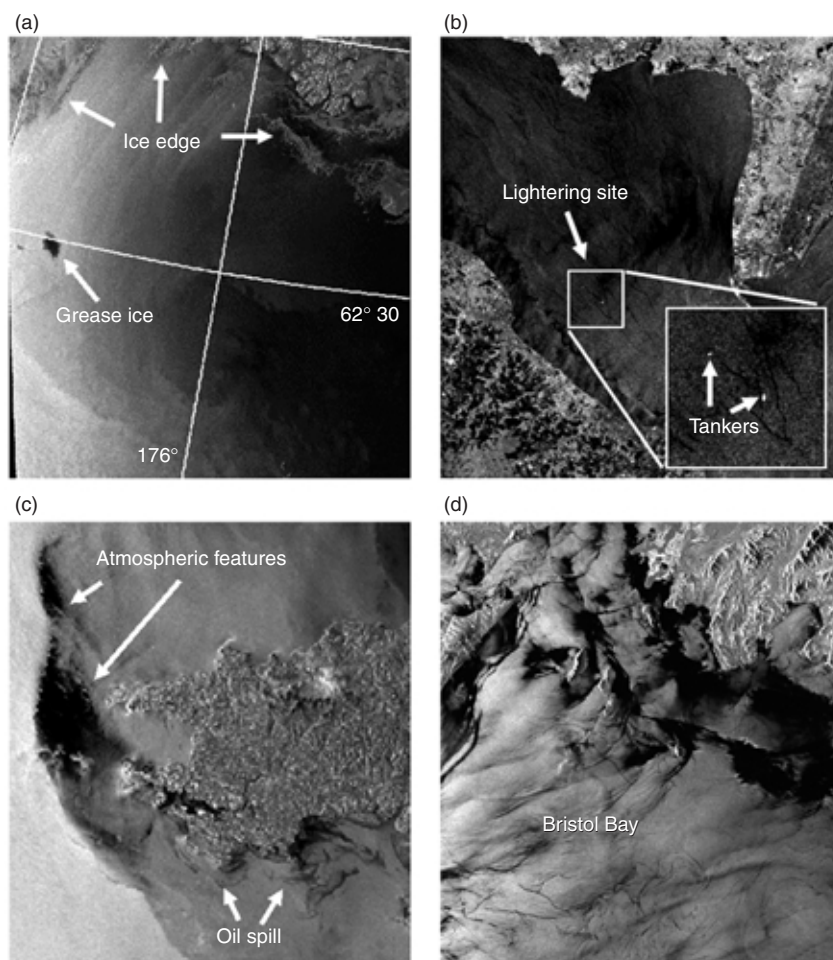


Figure 3. Additional image observations: (a) Radarsat ScanSAR wide subimage of the Bering Sea showing the presence of grease ice on 2 December 1998 at 0513 UT; (b) ERS-2 SAR image of the Delaware Bay showing slicks and the location of lightering activities on 14 May 1997 at 1543 UT; (c) ERS-1 SAR image acquired over Wales, UK, showing the *Sea Empress* oil slick and atmospheric patterns on 25 February 1996 at 2224 UT; and (d) ERS-1 SAR image of Bristol Bay, Alaska, showing ubiquitous meteorological and oceanographic low-backscatter features on 13 May 1994 at 0834 UT. (© Canadian Space Agency, 1998; © ESA, 1994, 1996, 1997.)

context, relation to other imaged features, and additional information provided by ancillary data. To date, the most thorough effort at characterizing these features has been done by the Nansen Environmental and Remote Sensing Center in Norway.⁹

The use of absolute NRCS values to distinguish among different low-backscatter phenomena appears at first to be a logical and appealing approach. Often, however, the use of the relative value or contrast between the low-backscatter features and the background in a scene is a more practical approach to their detection and characterization. This is particularly true since an absolute NRCS value requires a calibrated image. Once a low-backscatter feature has been detected, its morphological characterization as well as ancillary meteorological and oceanographic information can provide useful indications of its origin. Morphological characteristics of interest include the

shape, type of edge, texture, spatial extent, and variability of the feature. For example, the edges of low wind speed regions are usually less sharp than those of oil slicks.

Our ability to discriminate among different types of low-backscatter features is also aided by considering the geographical context of an image, for example, latitude (i.e., high versus low), proximity to the coast, coastal topography and geomorphology, and bathymetry. In addition, knowledge of activities typical to a region, such as fishing or oil operations, can further refine our judgment. Of course, care must be exercised when making assessments that heavily rely on such knowledge. Oil transfer operations, commonly referred to as lightering, are routinely conducted in the Delaware Bay to allow supertankers to navigate up the channel without running aground. Slicks resulting from biological activity blooms in the bay are also very common. Figure 3b shows an example of how natural slicks could easily be misinterpreted as man-made spills.

Knowledge of the temporal context of the image—including the time of day and season, as well as the persistence and development of a feature through multitemporal observations—is also invaluable.¹⁰

The presence of other features in an image also provides very useful insight to the interpretation of observed low-backscatter features. Such features may include atmospheric patterns like fronts or convective cells, the ice edge, or hard targets such as vessels, oil platforms, etc. Figure 3c shows the presence of large, low-backscatter features west of Wales at the time of the tanker *Sea Empress* oil spill. The features in the upper left are more than likely associated with meteorological processes along a strong atmospheric front rather than the presence of the oil spill that dominated the region in the lower right. Slicks extending from vessels are, for example, more likely to be of man-made than natural origin, although this is not always the case, as noted earlier.

Unfortunately, even after applying these characterization criteria, a completely unambiguous identification of almost any low-backscatter feature is not possible with the available one-band, one-polarization

satellite SAR sensors alone. The present sensor limitation is compounded by the simultaneous presence of different low-backscatter features in a scene. For example, meteorological and oceanographic feature signatures observed over the Bristol Bay in Alaska can add up to produce a relatively complicated image, as seen in Fig. 2d. Today, the best assessment of these features is attained when additional ancillary *in situ* and remote sensing data are available. These may include observations of meteorological conditions such as local wind speed and direction, air temperature, rain, and sea surface temperature. Ancillary data can be acquired by coastal weather stations, buoys, platforms, ships, satellites, or aircraft. The uncertainty in surfactant discrimination in particular could be greatly reduced if satellite and airborne visible and ultraviolet observations as well as actual shipboard microlayer sampling were available.

SUMMARY

Although the detection of a large number of low-backscatter ocean features is common in SAR imagery, their objective and unambiguous identification using satellite SAR sensors is not possible. The advent of a new generation of multiband and multipolarization SAR satellite systems should increase discrimination capabilities. For example, multiband and multipolarization SIR-C/X-SAR data have been shown to be useful in discriminating between biogenic and mineral surfactants.¹¹ The multisatellite SAR coverage expected to be operating at the beginning of the next century should also provide for much shorter revisit periods over areas of interest. This increased coverage is expected to enhance our ability to categorize many of these features by allowing additional information about their dynamics to be gained and used in their interpretation. It must still be recognized, however, that the best discrimination as well as the ultimate exploitation of the upcoming SAR systems will only be realized by proper integration of ancillary observations in the interpretation and analysis of the SAR data.

REFERENCES

- ¹Valenzuela, G. R., "Theories for the Interaction of Electromagnetic and Ocean Waves—A Review," *Boundary Layer Meteorol.* **13**, 61–85 (1978).
- ²Romeiser, R., Alpers, W., and Wismann, V., "An Improved Composite Surface Model for the Radar Backscattering Cross Section of the Ocean Surface I. Theory of the Model and Optimization/Validation by Scatterometer Data," *J. Geophys. Res.* **102**(C11), 25,237–25,250 (1997).
- ³Melsheimer, C., Alpers, W., and Gade, M., "Investigation of Multifrequency/Multipolarization Radar Signatures of Rain Cells over the Ocean Using SIR-C/X-SAR Data," *J. Geophys. Res.* **103**(C9), 18,867–18,884 (1998).
- ⁴Alpers, W., and Hühnerfuss, H., "The Damping of Ocean Waves by Surface Films: A New Look at an Old Problem," *J. Geophys. Res.* **94**, 6251–6265 (1989).
- ⁵Gade, M., Alpers, W., Hühnerfuss, H. H., Wismann, V. R., and Lange, P. A., "On the Reduction of the Radar Backscatter by Oceanic Surface Films: Scatterometer Measurements and Their Theoretical Interpretation," *Remote Sens. Environ.* **66**(1), 52–70 (1998).
- ⁶Friehe, C. A., Shaw, W. J., Rogers, D. P., Davidson, K. L., Large, W. G., et al., "Air-Sea Fluxes and Surface Layer Turbulence Around a Sea Surface Temperature Front," *J. Geophys. Res.* **96**, 8593–8609 (1991).
- ⁷Zheng, Q., Yan, X-H., Huang, N. E., Klemas, V., and Pan, J., "The Effects of Water Temperature on Radar Scattering from the Water Surface: An X-Band Laboratory Study," *Global Atmos. Ocean Sys.* **5**, 273–294 (1997).
- ⁸Gower, J. F. R., "Mapping of Surface Currents Using Naturally Occurring Surface Slicks Imaged by SAR," in *Proc. Second ERS-1 Symp.*, ESA SP-361, pp. 415–418 (1994).
- ⁹Hovland, H., A., Johannessen, J. A., and Digranes, G., "Slick Detection in SAR Images," in *Proc. IGARSS'94*, pp. 2038–2042 (1994).
- ¹⁰Clemente-Colón, P., Yan, X-H., and Pichel, W., "Evolution of Oil Slick Patterns as Observed by SAR off the Coast of Wales," in *Proc. 3rd ERS Symp.*, ESA SP-414, pp. 565–568 (1997).
- ¹¹Gade, M., Alpers, W., Hühnerfuss, H., Masuko, H., and Kobayashi, T., "The Imaging of Biogenic and Anthropogenic Surface Films by a Multi-Frequency Multi-Polarization Synthetic Aperture Radar Measured During the SIR-C/X-SAR Missions," *J. Geophys. Res.* **103**, 18,851–18,866 (1998).

ACKNOWLEDGMENTS: This article is based on work supported by the NOAA Ocean Remote Sensing (NORS) Program and the University of Delaware Sea Grant Office Program. Radarsat data were available through the NASA ADRO Project #396, ERS-1 through the PIPOR Proposal PI/BCB12, and ERS-2 through the ESA Project AO2USA136.

THE AUTHORS

PABLO CLEMENTE-COLÓN is affiliated with the NOAA/NESDIS Office of Research and Applications in Camp Springs, MD. His e-mail address is pablo.clemente-colon@noaa.gov.

XIAO-HAI YAN is with the College of Marine Studies at the University of Delaware, Newark. His e-mail address is xiaohai@udel.edu.